IOP Conf. Series: Materials Science and Engineering **202** (2017) 012021 doi:10.1088/1757-899X/202/1/012021

# Solid State Reaction Synthesis of Si-HA as Potential Biomedical Material: An Endeavor to Enhance the Added Value of Indonesian Mineral Resources

**Hartatiek, Yudyanto, S D Ratnasari, R Y Windari and N Hidayat**

[1]Department of Physics, Faculty of Mathematics and Natural Sciences, Universitas Negeri Malang (UM), Jl. Semarang 5, Malang 65145, Indonesia

Email: hartatiek.fmipa@um.ac.id

**Abstract**. In recent years, one of the most prominently investigated materials is hydroxyapatite (HA). It is because of its excellent properties for medical applications, essentially related to orthopedic. Also, the introduction of other materials to HA becomes another research focus of many leading scientists. In this present study, silicon with various concentrations was introduced, by means of solid state reaction route, to HA forming Si-HA. The crystal structure properties of the as-prepared samples were evaluated by X-ray diffractometer (XRD). Fourier Transform Infra Red (FTIR) spectroscopy data collection and analysis were done to investigate the functional groups within the samples. The microstructural characteristics as well as elemental mapping of the samples were captured by scanning electron microscopy and energy dispersive x-ray spectroscopy (SEM-EDX). Vickers hardness test was also conducted to investigate the hardness properties of the samples. Furthermore, *in vitro* characterization-based bio resorbability of the samples in a simulated body fluid were also described. This study revealed that Indonesian limestone can be utilized as the raw material for synthesizing HA. The silicon has been successfully incorporated into phosphate site of the HA crystal. Conclusively, the Si-HA reported in this study shows good bioresorbability characteristic.

**Keywords**: Si-HA, solid state reaction, biomedical material.

## 1. Introduction

Study of biomedical materials for bone implantation has been extensively made for the last decades. One of the most securing materials for bone repair and bone regeneration is the well-known hydroxyapatite ($Ca_{10}(PO_4)_6(OH)_2$, HA) [1,1] that is attributable to its resemblance to the human bone [2,3]. Many approaches have been conducted to produce HA, for instance by means of hydrothermal [4], sol-gel precipitation [5], ultrasound irradiation [6], and microwave-assisted approaches [7]. In addition, solid-state reaction technique is, in spite of everything, recognized as one of the most effective methods for HA production [8–11]. However, a study exclusively investigating the use of natural calcium-based materials to synthesize HA is rarely conducted. This breakthrough is important not only to reduce the cost of HA production but also to provide an added-value of the abundant natural resources, i.e. limestone.

Limestone is one of the most abundantly naturally-occurring minerals [12] consisting mainly of calcium carbonate ($CaCO_3$) in three different crystalline phases, i.e. calcite, vaterite, and aragonite [12,13]. It is captivating to know the way the nature adeptly models and accurately organizes the

building block, constituent composition, polymorphism, and other remarkable characteristics of $CaCO_3$. Previous study showed that high-purity $CaCO_3$ could be found in many sites in Indonesia [14]. However, it becomes less valuable due to its unnecessary purposes of exploitation. This work, then, introduces the possibility of realizing a beneficial use of limestone as the calcium stand-in to fabricate calcium phosphate-based HA.

Eventhough HA offers outstanding osteoconductivity and biocompatibility [15], pure-HA, at the same time, performs low reactivity with the original (human) bone [16] leading to insufficient ability to create interfaces with the original bone and to stimulate the new bone formation [17]. So, having succeeded in producing pure-HA may not solve the challenge of creating an excellent biomedical material for bone grafting yet.

The best way to solve this problem is to modify HA crystal structure with insertion of small amount of silicon. Silicon is frequently used as dopant for bioceramics since it significantly enhances the ultimate properties of the biomaterials such as surface chemical structure, mechanical strength, bioactivity, and biocompatibility [17]. Particularly, silicon plays an important role at the early stages in stimulating normal growth of bone and soft tissue development [18]. Therefore, in this work, we report the use of limestone in HA production by means of solid state reaction and study the effect silicon on the characteristics of silicon-doped hydroxyapatite (Si-HA).

## 2. Experimental Method

A limestone from Malang, Indonesia, was selected prior to produce HA. The limestone was grounded and sieved. Only particles passing a mesh screen with 200 mesh were used in this study. The powder was calcined at1000 °C for 5 h to obtain CaO powder. The CaO was then dissolved in distilled water. $H_3PO_4$ (Sigma-Aldrich) was added to the CaO solution and stirred at 30 °C for 30 min. Filtration was made after stirring the solution. The precipitate was heated at 700 °C for 10 h to form calcium phosphate, $Ca_2P_2O_7$. The primary materials to synthesize Si-HA were prepared after the stoichiometric calculation, i.e. $CaCO_3$ from limestone, $Ca_2P_2O_7$, and $SiO_2$ (Sigma-Aldrich). These materials were mixed and grounded for 30 h followed by pressing to produce cylindrical-shaped samples. The as-prepared samples were sintered at 1100 °C for 20 h. The characterizations were performed by means of XRD for crystal structure and phase content study. The microstructural investigation and elemental mapping of the samples were conducted by using Scanning Electron Microscopy (SEM) and energy dispersive x-ray (SEM-EDX). Furthermore, Vickers hardness tes was used to study the mechanical strength od the samples. The functional groups of the samples were determination by using Fourier-Transform Infrared (FTIR).

## 3. Results and Discussion

The previous study [19] revealed that the content of calcium from the limestone was above 97%. The diffraction profile of the as-prepared calcium phosphate also depicted that the crystal structure was in good agreement with the crystallographic open database code 96-200-1133. It implies that the limestone can be well used as the raw material to produce calcium phosphate and for further used for the production of HA.

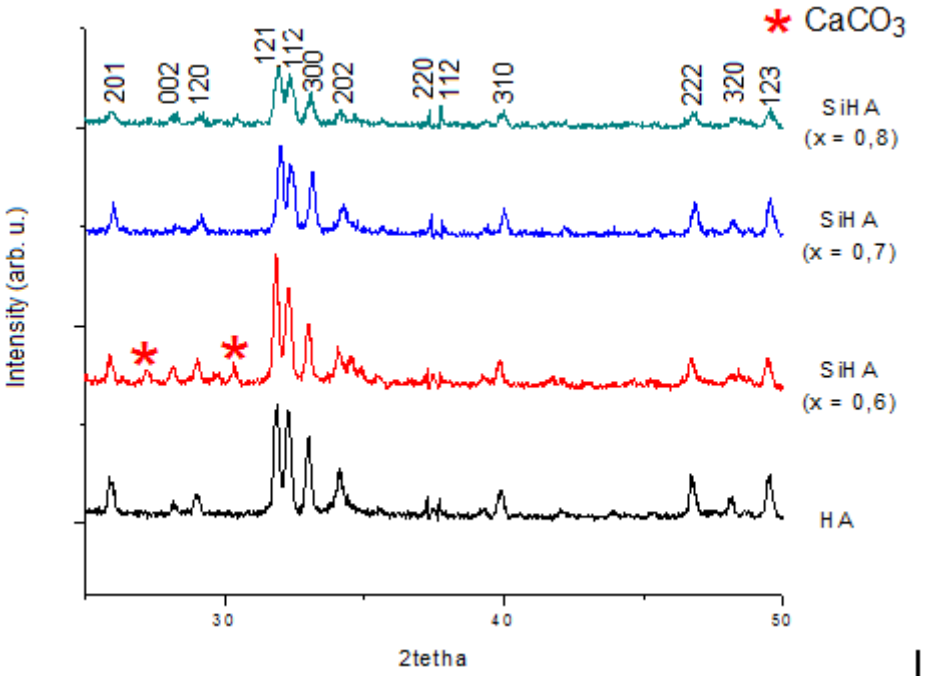


**Figure 1.** XRD profiles of pure-HA and Si-HA with various Si contents

The XRD data for Si-HA with various Si contents can be viewed in Figure 1. There is no peak found in which corresponding to silicon. The arrangement of 2-theta and intensities of the XRD profiles, particularly for pure-HA refers to the crystal structure of hydroxyapatite with the PDF reference code of 01-084-1998 without the presence of any minor phases. Introducing of silicon to HA does not change the XRD patterns, meaning that the crystal structures remain unchanged. Even if there is a lattice distortion, it will be very insignificant [15]. Only Si-HA with $x = 0.6$ containing additional peaks referring to aragonite $CaCO_3$ with the PDF code of 00-024-0025. The hydroxyapatite detected in the XRD patterns has hexagonal crystalline system with space group of P63/m. The absence of silicon-containing XRD peaks implies that the silicon might successfully incorporate to HA sites.

Further XRD data analysis was conducted to explore degree of crystallinity as well as crystalline size. The crystalline size was evaluated by means of Scherrer equation [20]. Since, in principle, the equation which based on the XRD peak broadening can be applied to predict the size of crystal [21]. The crystalline size of Si-HA with silicon contents of 0, 0.6, 0.7, and 0.8 are 26.85 nm, 34.85 nm, 40.06 nm, and 40.84 nm, respectively. These results are in a good agreement with another report [15]. In other words, there is an increasing size of crystal for silicon-containing HA with respect to the concentration of silicon. On the other side, crystallinity of the samples also varies with different silicon content. The crystallinities of Si-HA with silicon contents of 0, 0.6, 0.7, and 0.8 are 35.75%, 29.40%, 21.66%, and 20.99%, respectively. The reduced of the degree of crystallinity is strongly believed that it is due to the incorporation of $SiO_4^{4-}$ ions into HA sites by exchanging $PO_4^{3-}$ ions [22].

One of the most important characteristics of HA is the ratio of Ca/P or Ca/(P + Si) for Si-HA. Therefore, here we also report the ratio by means of SEM-EDAS measurement. Figure 2 shows the SEM-EDAS elemental analysis of Si-HA with $x = 0.6$ (data for pure-HA and other Si-HAs are not shown). From Figure 2, we can calculate the ratio of Ca/(P + Si) is 1.80. The ratio of Ca/P for pure-HA is 1.67 which is very close to the ratio reported by other researchers [20–24]. Figure 3 represents the microstructure of pure-HA and Si-HA. It informs us that there is a significant decrease of porosity as the increase of silicon contents. Quantitatively, the porosity of sample reduces from 10.27% (pure-HA) to 8.97% ($x = 0.6$), 7.69% ($x = 0.7$), and 7.60% ($x = 0.8$). The decrease of porosity reveals that the

incorporation of silicon into HA takes place the pore of the system. This case may assist dissolution of surface ions that stimulates the formations of apatite layer [17].

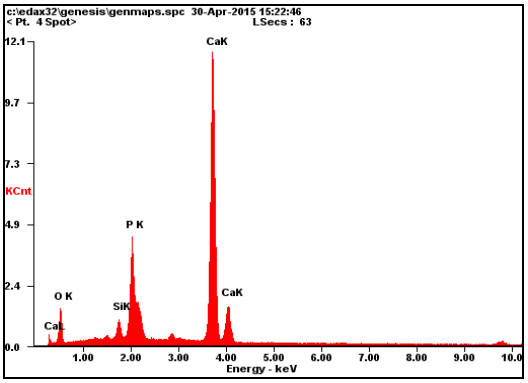


| Element | Wt% | At% |
|---|---|---|
| O | 30.58 | 50.84 |
| Si | 01.93 | 01.82 |
| P | 13.04 | 11.20 |
| Ca | 54.45 | 36.14 |

**Figure 2.** SEM-EDAS elemental analysis of Si-HA ($x = 0.6$)

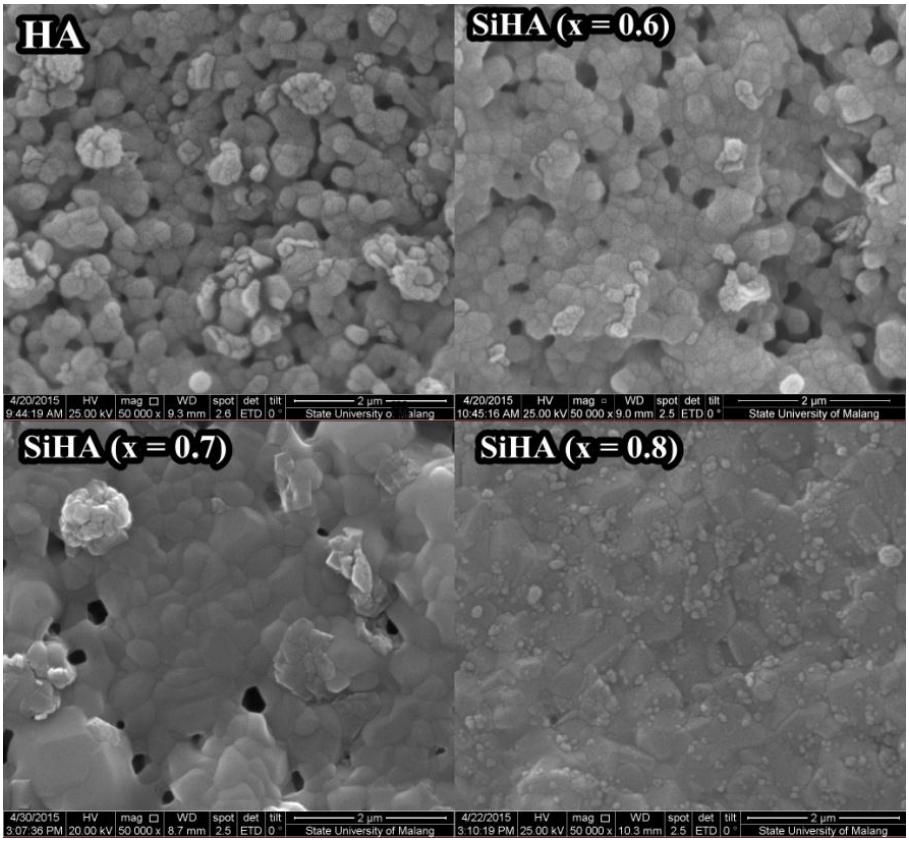


**Figure 3.** SEM photographs of pure-HA and Si-HA

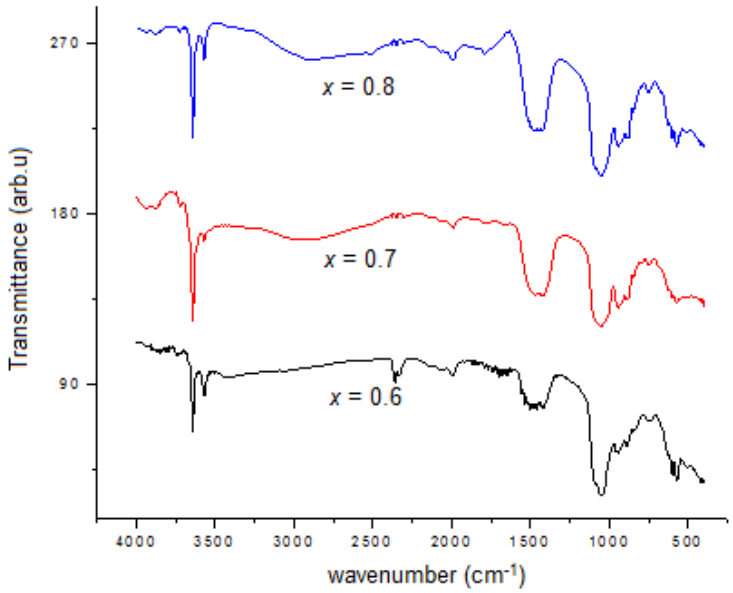


**Figure 4.** FTIR Spectra of Si-HA with different silicon concentrations

FTIR was applied to investigate the influence of the Si incorporation on the different functional groups of Si-HA. From Figure 4, Asymmetric bending vibration of $PO_4^{3-}$ groups is precieved at 570 $cm^{-1}$ [27]. Another phosphate bonding is also noted at 601 $cm^{-1}$ [28]. Hydroxyl group bending is found in 630 $cm^{-1}$ [5]. Si-O and P-O stretching, which decrease and become less resolved as the higher amount of silicate content [1], are shown by the FTIR bands in 950 $cm^{-1}$ and [1,15] and 1089 $cm^{-1}$ [15]. Hydroxyapatite broad absorption corresponding to $PO_4^{3-}$ stretching vibrational mode is discovered at 900-1100 $cm^{-1}$ [29]. In addition, silicate and phosphate tetrahedral molecular units share several similarities of asymmetrical stretching vibration modes in the range of 900-1100 $cm^{-1}$ [1]. Increase in broadening peak at 1060 $cm^{-1}$ is strongly believed as the incorporation of silicon and the decrease of crystallinity [22]. Asymmetric stretching of $CO_3^{2-}$ groups is detected at 1400 $cm^{-1}$ [27]. Hydroxyl group stretching in hexagonal channels and surface hydroxyl group are observed at 3572 $cm^{-1}$ [5] and 3643 $cm^{-1}$ [22].

The hardness characteristic of the Si-HA was characterized by means of Vickers hardness test. It is revealed that the addition of silicon into hydroxyapatite elevates the hardness. Figure 5 represents the graph that contains information on the interconnection between hardness and porosity of Si-HA.

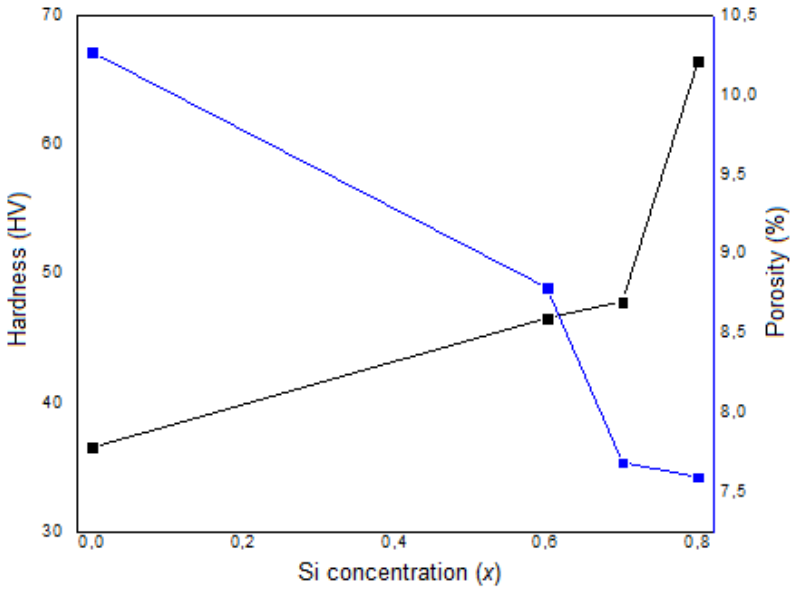


**Figure 5.** Hardness and porosity characteristics of Si-HA with different silicon concentrations

The high temperature sintering applied during the synthesis may give chance for the grains to grow due to the densification process [30]. Introducing silicon into hydroxyapatite yields the reduction of porosity, meaning that the Si-HA becomes denser as the quantity of silicon intensifies. Which in turns, it increases the hardness value of the prepared Si-HA.

Furthermore, the bioresorbability of the sample with the lowest silicon concentration in Si-HA prepared in the series of this experiment was evaluated by means of immersing the sample in simulated body fluid (SBF) solution for hours. Bioresorbance is one of biodegradation phenomena indicated by the decrease of mass during the immersion of sample in a fluid [31]. It can be evaluated by calculating the mass reduction of Si-HA in SBF solution. The average mass reduction of Si-HA per day was 0.003 g. It implies that the Si-HA is applicable for biomedical applications [31].

## 4. Conclusion

The present work describes the characteristics of Si-HA prepared by solid-state reaction approach. It is discovered that the limestone from Indonesian mineral resource can be effectively used as the raw-material for hydroxyapatite production. The XRD data revealed the absence of silicon-oxide-based diffraction peaks and FTIR spectra convincing the presence of Si-O functional groups. It implies that the silicon has been successfully inserted into phosphate site within the crystal of hydroxyapatite. The Vickers hardness of the samples increased as the decrease of porosity. Finally, the produced Si-HA shows the feasibility for biomedical applications particularly due to its bioresorbability characteristic.

## 5. References

[1] Padmanabhan S K, Ul Haq E and Licciulli A 2014 Rapid synthesis and characterization of silicon substituted nano hydroxyapatite using microwave irradiation *Curr. Appl. Phys.* **14** 87–92

[2] Rodríguez-Valencia C, López-Álvarez M, Cochón-Cores B, Pereiro I, Serra J and González P 2013 Novel selenium-doped hydroxyapatite coatings for biomedical applications *J. Biomed. Mater. Res. A* **101A** 853–61

[3] Marchat D, Bouët G, Lueckgen A, Zymelka M, Malaval L, Szenknect S, Dacheux N, Bernache-Assollant D and Chevalier J 2013 Physico-Chemical Characterization and In Vitro

Biological Evaluation of Pure SiHA for Bone Tissue Engineering Application *Key Eng. Mater.* **529–530** 351–6

[4] Zhang C, Yang J, Quan Z, Yang P, Li C, Hou Z and Lin J 2009 Hydroxyapatite Nano- and Microcrystals with Multiform Morphologies: Controllable Synthesis and Luminescence Properties *Cryst. Growth Des.* **9** 2725–33

[5] Sanosh K P, Chu M-C, Balakrishnan A, Lee Y-J, Kim T N and Cho S-J 2009 Synthesis of nano hydroxyapatite powder that simulate teeth particle morphology and composition *Curr. Appl. Phys.* **9** 1459–62

[6] Brundavanam S, Poinern G E J and Fawcett D 2015 Synthesis of a Hydroxyapatite Nanopowder via Ultrasound Irradiation from Calcium Hydroxide Powders for Potential Biomedical Applications *Nanosci. Nanoeng.* **3** 1–7

[7] Amer W, Abdelouahdi K, Ramananarivo H R, Zahouily M, Fihri A, Djessas K, Zahouily K, Varma R S and Solhy A 2013 Microwave-assisted synthesis of mesoporous nano-hydroxyapatite using surfactant templates *CrystEngComm* **16** 543–9

[8] Pramanik S, Agarwal A K, Rai K N and Garg A 2007 Development of high strength hydroxyapatite by solid-state-sintering process *Ceram. Int.* **33** 419–26

[9] Ingole V H, Hussein K H, Kashale A A, Gattu K P, Dhanayat S S, Vinchurkar A, Chang J-Y and Ghule A V 2016 Invitro Bioactivity and Osteogenic Activity Study of Solid State Synthesized Nano-Hydroxyapatite using Recycled Eggshell Bio–waste *ChemistrySelect* **1** 3901–8

[10] Guo X, Yan H, Zhao S, Li Z, Li Y and Liang X 2013 Effect of calcining temperature on particle size of hydroxyapatite synthesized by solid-state reaction at room temperature *Adv. Powder Technol.* **24** 1034–8

[11] Aina V, Cerrato G, Martra G, Bergandi L, Costamagna C, Ghigo D, Malavasi G, Lusvardi G and Menabue L 2013 Gold-containing bioactive glasses: a solid-state synthesis to produce alternative biomaterials for bone implantations *J. R. Soc. Interface* **10** 20121040

[12] Meddah M S, Lmbachiya M C and Dhir R K 2014 Potential use of binary and composite limestone cements in concrete production *Constr. Build. Mater.* **58** 193–205

[13] Fujiwara M, Shiokawa K, Araki M, Ashitaka N, Morigaki K, Kubota T and Nakahara Y 2010 Encapsulation of Proteins into CaCO3 by Phase Transition from Vaterite to Calcite *Cryst. Growth Des.* **10** 4030–7

[14] Hidayat N, Ramli I, Sunaryono S, Taufiq A, Zainuri M and Pratapa S 2015 Gradualisme Struktur Kristal dan Sifat Mekanik Material Fungsional Kalsit-Mg/Al Hasil Fabrikasi dengan Metode Infiltrasi Seminar Nasional Fisika dan Pembelajarannya 2015 (Malang: Department of Physics, UM) p FM19-FM24

[15] Rau J V, Fosca M, Cacciotti I, Laureti S, Bianco A and Teghil R 2013 Nanostructured Si-substituted hydroxyapatite coatings for biomedical applications *Thin Solid Films* **543** 167–70

[16] Ducheyne P, Radin S and King L 1993 The effect of calcium phosphate ceramic composition and structure on in vitro behavior. I. Dissolution *J. Biomed. Mater. Res.* **27** 25–34

[17] Khan A F, Saleem M, Afzal A, Ali A, Khan A and Khan A R 2014 Bioactive behavior of silicon substituted calcium phosphate based bioceramics for bone regeneration *Mater. Sci. Eng. C* **35** 245–52

[18] Hing K A, Revell P A, Smith N and Buckland T 2006 Effect of silicon level on rate, quality and progression of bone healing within silicate-substituted porous hydroxyapatite scaffolds *Biomaterials* **27** 5014–26

[19] Hartatiek H, Yudyanto Y, Windari R Y, Ratnasari S D and Hidayat N 2016 Karakteristik Hidroksiapatit Doping Silikon Si0,5HA Hasil Reaksi Keadaan Padat dan Potensinya sebagai Material Biomedis Seminar Fisika dan Pembelajarannya 2016 (Malang: Jurusan Fisika UM)

[20] Scherrer P 1918 Determination of the size and internal structure of colloidal particles using X-rays *Math-Phys Kl.* **2** 98–100

[21] Hidayat N, Sunaryono S and Taufiq A 2016 Komparasi Analisis Ukuran Kristal Partikel Nano Magnetit Berbasis Data Difraksi Sinar-X dengan Beragam Metode Seminar Fisika dan Pembelajarannya 2016 (Malang: Jurusan Fisika UM)
[22] Sutha S, Kavitha K, Karunakaran G and Rajendran V 2013 In-vitro bioactivity, biocorrosion and antibacterial activity of silicon integrated hydroxyapatite/chitosan composite coating on 316 L stainless steel implants *Mater. Sci. Eng. C* **33** 4046–54
[23] Jeong Y-H, Kim J-J and Choe H-C 2016 Surface Characteristics of Nano-Structured Silicon/Hydroxyapatite Deposition onto the Ti–Nb–Zr Alloy *J. Nanosci. Nanotechnol.* **16** 1783–6
[24] Harden F J, Gibson I R and Skakle J M S 2013 Simplification of the Synthesis Method for Silicon-Substituted Hydroxyapatite: A Raman Spectroscopy Study *Key Eng. Mater.* **529–530** 94–9
[25] Surmeneva M A, Surmenev R A, Chaikina M V, Kachaev A A, Pichugin V F and Epple M 2013 Phase and elemental composition of silicon-containing hydroxyapatite-based coatings fabricated by RF-magnetron sputtering for medical implants *Inorg. Mater. Appl. Res.* **4** 227–35
[26] Yu H, Liu K, Zhang F, Wei W, Chen C and Huang Q 2015 Microstructure and in vitro Bioactivity of Silicon-Substituted Hydroxyapatite *Silicon* 1–11
[27] López-Álvarez M, Solla E L, González P, Serra J, León B, Marques A P and Reis R L 2009 Silicon–hydroxyapatite bioactive coatings (Si–HA) from diatomaceous earth and silica. Study of adhesion and proliferation of osteoblast-like cells *J. Mater. Sci. Mater. Med.* **20** 1131–6
[28] Kannan S, Lemos A F and Ferreira J M F 2006 Synthesis and Mechanical Performance of Biological-like Hydroxyapatites *Chem. Mater.* **18** 2181–6
[29] Bianco A, Cacciotti I, Lombardi M and Montanaro L 2009 Si-substituted hydroxyapatite nanopowders: Synthesis, thermal stability and sinterability *Mater. Res. Bull.* **44** 345–54
[30] Barsoum M and Barsoum M W 2002 *Fundamentals of Ceramics* (CRC Press)
[31] Rameshbabu N and Rao K P 2009 Microwave synthesis, characterization and in-vitro evaluation of nanostructured biphasic calcium phosphates *Curr. Appl. Phys.* **9** S29–31